One potential drawback of the excitation geometry presented here is that the metal-coated gratings used in dye lasers have relatively low damage thresholds and hence are susceptible to damage by the pump laser. However, this is not a serious limitation especially in dye laser systems of the oscillator amplifier type, in which the oscillator is pumped with a small amount of pump energy to obtain a narrow spectral linewidth. In addition, the large magnification of the pump beam on the grating surface that is due to the grazing incidence results in a considerable reduction in power density. In our laser system we have not encountered grating damage over several weeks of operation. For oscillator amplifier systems, it is desirable to obtain emission with good spatial quality from the oscillator and in this respect the present pumping arrangement may be more attractive than off-axis pumping because of a better match of the pump laser and the dye laser modes.

To summarize, a new pumping geometry for a grazing-incidence grating dye laser has been presented in which true longitudinal pumping is achieved by coupling the pump beam to the dye laser resonator by way of zero-order diffraction from the grating. Laser emission with good spatial quality was obtained from a dye laser based on this configuration.

The authors thank M. Laghate for technical assistance, S. M. Oak and H. S. Vora for help during the experiments, and K. C. Rustagi for a critical reading of the manuscript.

References

1. P. P. Sorokin, J. R. Lankard, E. C. Hammond, and V. L. Moruzzi, "Laser pumped stimulated emission from organic dyes: experimental and analytical comparisons," IBM J. Res. Dev. **11,** 130–147 (1967).
2. F. J. Duarte, "Technology of pulsed dye lasers," in *Dye Laser Principles,* F. J. Duarte and L. W. Hillman, eds. (Academic, San Diego, 1990), pp. 239–285.
3. M. G. Littman and H. J. Metcalf, "Spectrally narrow pulsed dye laser without beam expander," Appl. Opt. **17,** 2224–2227 (1978).
4. I. J. Wilson, B. Brown, and E. G. Loewen, "Grazing incidence grating efficiencies," Appl. Opt. **18,** 426–427 (1979).

Sun photometer with light-emitting diodes as spectrally selective detectors

Forrest M. Mims III

The author is with Science Probe, Inc., 433 Twin Oak Road, Seguin, Texas 78155.
Received 21 February 1992.
0003-6935/92/336965-03$05.00/0.

Light-emitting diodes can function as spectrally selective detectors in a miniature, inexpensive sun photometer that measures atmospheric turbidity and precipitable water.

Key words: *Light-emitting diode, ozone, precipitable water, sun photometer, turbidity.*

Light-emitting diodes (LED's) can function as light detectors with a spectral bandpass similar to the diode's spectral emission band,[1] typically 25–35 nm at the half-maximum points. This means that LED's can serve as detectors in miniature sun photometers that measure precipitable water and atmospheric turbidity at wavelengths from 555 to 940 nm.

LED's are much smaller and sturdier than photodiodes fitted with interference filters. LED's that respond to 20–30-nm bands between 555 and 700 nm and 50–100-nm bands between 850 and 950 nm are available for less than 1% of the cost of a photodiode with a 10-nm bandpass interference filter. The solar photocurrent from some LED's with an integral lens is so high (>10 μA) that no electronic amplification is required. However, lensless LED's are preferred since heating that might be caused by concentrated sunlight can shift spectral sensitivity (0.13 nm/°C for AlGaAs visible emitters[1]).

I have designed and am now evaluating a handheld, six-channel LED sun photometer with a digital display for the Science Probe Atmospheric Network, a program designed to provide inexpensive meteorological instruments to scientists, students, and other observers in developing countries. The sensor for this miniature (5 cm × 10 cm × 2.5 cm; 130 g) instrument is 6 LED chips (Table 1) that are installed on a common substrate (Fig. 1) and that view the sun through an aperture, giving a field of view of <3 deg. Six such detector arrays were fabricated for this investigation by Marktech International Corporation (5 Hemlock Street, Latham, New York 12110). The LED dies were not installed on reflective headers of the kind used for most commercial LED's in order to reduce the amount of radiation that enters the edge of the *pn* junction and that otherwise broadens their detector-mode spectral bandpass. The photocurrents from the LED's are amplified by an operational amplifier with switch-selectable gains of 10^3 and 10^4. The circuit is identical to that of an ultraviolet photometer described elsewhere.[2]

The Langley plots in Fig. 2 affirm that the logs of the solar photocurrent from the LED's are nearly linear with respect to an air mass over a wide range of air masses, a prerequisite for spectrally selective, direct sun photometry. The observations were made near Seguin, Texas (29° 35′N 97° 58′W) on Dec. 28, 1991. Although the sky was clear, a bright solar corona indicated the presence of aerosols from the eruption of Mt. Pinatubo on June 15, 1991. The logs of the photocurrents from the 880- and 940-nm LED's have been adjusted by a constant (+0.3 and −0.2, respectively) to eliminate overlapping. The shift in response of the 940-nm LED in Fig. 2 was caused by changes in column water vapor.

Table 1. Peak Wavelength Emission and Bandwidth of LED's Used as Detectors in a Sun Photometer

Composition of LED Die	Peak Emission Wavelength (nm)[a]	Emission Bandwidth (nm)[b]
GaP–GaP	555 (green)	25
GaAsP–GaP	610 (orange)	35
GaAlAs–GaAlAs	660 (red)	25
GaAlAs–GaAs	700 (red)	25
GaAlAs–GaAlAs	880 (near IR)	80
GaAs–GaAs	940 (near IR)	45

[a]Peak emission wavelength and emission bandwidth as specified by the manufacturer of the LED die.
[b]Spectral emission bandwidth at FWHM.

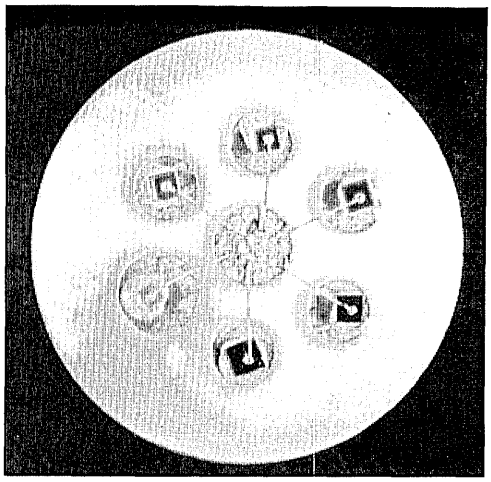

Fig. 1. Six-element spectrally selective LED detector array.

The lines through the points in Fig. 2 are best fits for the function $y = a + bx$, as computed by TableCurve™ (Jandel Scientific). The correlation coefficient r exceeds 0.99 for each LED. The lines through the points have been extended to an air mass m of 0 to give the extraterrestrial constant I_0 for each LED. The slope of each line represents the atmospheric optical thickness (AOT) at each wavelength. AOT at a specific wavelength (including Rayleigh, aerosol, and gas absorber thickness) is the product of m and the difference between the natural logs of I_0 and the measured signal. (A method for computing AOT is given by Volz.[3])

Before the LED detector array was specified, the ability of LED's to detect precipitable water was tested. It was found that a 940-nm GaAs:Si LED can detect the 940-nm water-vapor absorption band sufficiently well to be paired with an AlGaAs LED that emits, and therefore detects, at 880 nm, thereby forming a simple near-infrared hygrometer. Figure 3 compares the ratio of photocurrents from a 940-nm LED and an 880-nm LED with precipitable water for all 228 observations during 1990–1991 in a manner used to calibrate infrared hygrometers.[4,5] Precipitable water was computed from the surface dew point.[6] The uppermost data point on the y axis in Fig. 3 is the mean of 11 observations made through a clean window of a commercial aircraft at an altitude of 11.9 km (LED photocurrent ratio = 0.619; standard deviation = 0.015). For the purpose of this work, precipitable water at this altitude is assumed to be 1 mm.

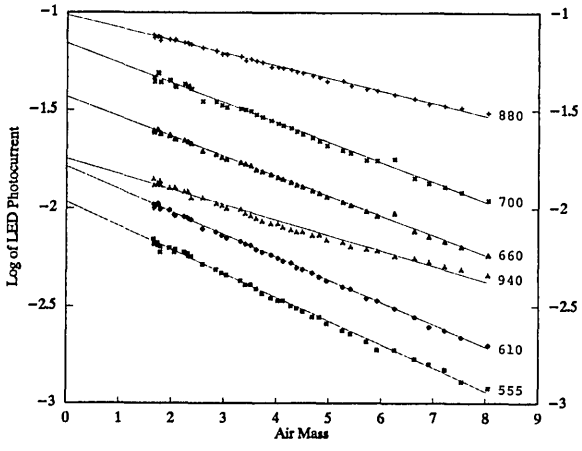

Fig. 2. Langley plot for each channel of a LED sun photometer.

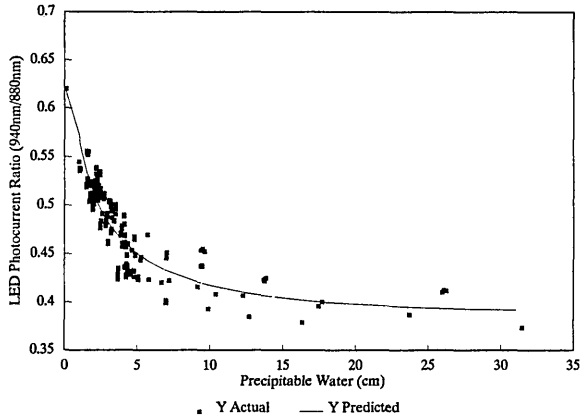

Fig. 3. LED hygrometer calibration curve.

The function of the data plotted in Fig. 3 is approximated by the exponential expression

$$y = 0.4 + 0.21 \exp(-x/3.05), \tag{1}$$

where y is the ratio of the LED photocurrents and x is precipitable water (cm). The chief drawback of Eq. (1) is that y levels off when $x > 15$ cm. This is corrected in Fig. 3, in which the curve drawn through the points is given by

$$y = 0.57 + 0.014(\ln x)^2 + 0.098 \ln x + 0.011 \ln x/x. \tag{2}$$

Equation (2) gives an insignificantly lower correlation coefficient than does Eq. (1) ($r = 0.896$ and 0.9, respectively).

Surprisingly, the LED sun photometer method gives somewhat higher values of r than those for two hygrometers I designed that employ Si photodiodes and narrow bandpass (10 nm at the half-maximum points) interference filters (940 and 1003 nm, $r = 0.89$, and 940 and 850 nm, $r = 0.85$). A possible explanation for the superior performance of the LED detectors is that temperature changes shifted the transmission of the 940-nm filters with respect to the water-vapor absorption line. The peak spectral response of a typical 940-nm LED increases ~0.28 nm/°C while the peak transmission wavelength of a typical interference filter increases only ~0.02 nm/°C. Temperature changes might have less effect on the 940-nm LED since its bandpass is ~5 times wider than that of the filters.

In principle, a standard two-chip, bicolor, orange–red (610 and 660 nm) LED can detect ozone by observing the Chappuis absorption band at 610 nm, the 660-nm LED being the reference detector. While the low-absorption cross section of the Chappuis band limits the accuracy of this method, especially when the air mass is near unity, preliminary indications are that LED's can detect ozone sufficiently well to indicate seasonal trends if observations are made when the air mass is >3. Preliminary results also show that the sun photometer can be used aboard a commercial aircraft to sense the difference in column ozone between the surface and an altitude of >10 km.

A long-term comparison of observations of precipitable water, AOT, and ozone made with the LED sun photometer and photometers equipped with interference filters began in December, 1991, and is ongoing. Results of this study will be submitted for publication later. It is expected that the calibration of the precipitable water detection mode will be improved by comparing observations with those made during the flights of radiosondes. Precipitable water will also be computed by using Beer's law and the I_0 measured during aircraft flights. Other applications for LED's as spectrally selective detectors now being investigated include miniaturized transmission and reflection spectrometers that fit in a pocket and are rugged enough for field use.

I thank Vince Forte and Kevin Ward of Marktech International for their prompt assistance in fabrication of the LED detector assemblies and two anonymous reviewers for helpful suggestions.

References

1. R. Lynch, *The Role of Compositionally Graded GaAlAs Diodes in Optical Communications* (IBM Electronics Systems Center, New York, 1972).
2. F. M. Mims, III, "How to monitor ultraviolet radiation from the sun," Sci. Am. **263,** 106–109 (1990).
3. F. Volz, *Sun Photometer* (Volz, Lexington, Mass., 1990).
4. N. Foster and L. Foskett, "A spectrophotometer for the determination of the water vapor in a vertical column of the atmosphere," J. Opt. Soc. Am. **35,** 601–610 (1945).
5. C. Tomasi and R. Guzzi, "High precision atmospheric hygrometry using the solar infrared spectrum," J. Phys. E **7,** 647–649 (1974).
6. C. Reitan, "Surface dew point and water vapor aloft," J. Appl. Meteorol. **2,** 776–779 (1963).

Technique to determine dominant radiative processes in low-pressure rare gas lasers

Shane A. Brunker and Kenneth J. Grant

The authors are with the Electronics Research Laboratory, Defence Science and Technology Organisation, P.O. Box 1500, Salisbury, South Australia 5108, Australia.

Received 25 February 1992.
0003-6935/92/336967-03$05.00/0.

We describe a technique to determine dominant radiative processes in rare gas lasers, with application to the He–Xe laser.

Recently there has been a significant increase in research on atomic rare gas lasers as a result of their high gain and large output powers.[1–3] These lasers are usually run at medium to high discharge pressures (0.5–16 atm) with an *e*-beam sustained discharge. Low-pressure (0.01–0.03 atm) longitudinally excited discharge lasers, although of much lower output powers and efficiencies, have a high degree of flexibility in producing output powers that have temporal profiles ranging from cw to 10 kHz over a broad range of wavelengths.[4] Interpretation of the temporal output waveforms usually requires access to voluminous transition probability data, followed by extensive calculations of energy level lifetimes and branching ratios. We report here the application of a database program to the results obtained from an atomic He–Xe rare gas laser to determine possible dominant radiative processes occurring within low-pressure discharge during lasing. (A complete model of the discharge would also require an estimation of the effects from two- and many-body collisions, particularly at higher pressures.[5,6])

The apparatus used to obtain the lasing lines has been described elsewhere.[4] In summary, the laser consists of a longitudinal discharge operating at a pressure of 20 Torr and a He:Xe partial pressure ratio of between 80:1 and 120:1, and is line tuned by using a diffraction grating as one of the cavity reflectors. The laser output is monitored by recording the voltage output from a PbSe sensor (Opto-Electronics, model OTC-12S-81T). The signal was digitized and stored on an XT-compatible computer.

Two lasing lines of particular interest are the 3.894 and 3.995 μm because of their spectral position within one of the atmospheric windows. These lines result from an inversion between the $5d[7/2]_3$ and $6p[5/2]_3$ states (3.894 μm), and the $5d[1/2]_0$ and $6p[1/2]_1$ states (3.995 μm). When the laser is operating in a modulated mode, the temporal profile of the 3.894-μm line closely follows the shape of the square excitation current pulse, as shown in Fig. 1. In contrast, however, the 3.995-μm line exhibits a profile that is dissimilar to that of the current, with the

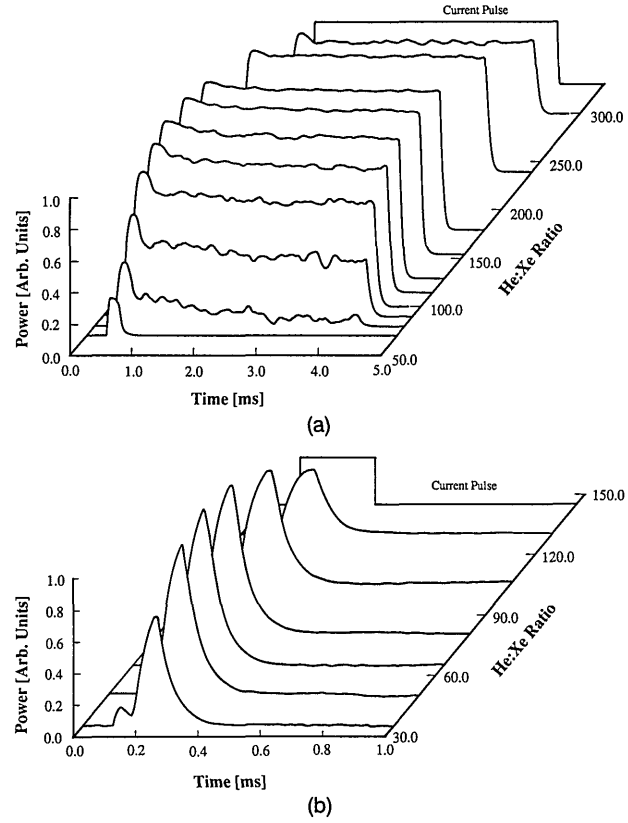

Fig. 1. Temporal profiles at a range of He:Xe partial pressure ratios for (a) the 3.894-μm and (b) the 3.995-μm laser lines.